Chemical Science

Cite this: *Chem. Sci.*, 2012, **3**, 1707

www.rsc.org/chemicalscience

EDGE ARTICLE

Lanthanide ions as required cofactors for DNA catalysts†

Victor Dokukin and Scott K. Silverman*

Received 16th December 2011, Accepted 1st March 2012
DOI: 10.1039/c2sc01067d

We report that micromolar concentrations of lanthanide ions can be required cofactors for DNA-hydrolyzing deoxyribozymes. Previous work identified deoxyribozymes that simultaneously require both Zn^{2+} and Mn^{2+} to achieve DNA-catalyzed DNA hydrolysis (10^{12} rate enhancement); a mutant of one such DNA catalyst requires only Zn^{2+}. Here we show that *in vitro* selection in the presence of 10 μM lanthanide ion (Ce^{3+}, Eu^{3+}, or Yb^{3+}) along with 1 mM Zn^{2+} leads to numerous DNA-hydrolyzing deoxyribozymes that strictly require the lanthanide ion as well as Zn^{2+} for catalytic activity. These DNA catalysts have a range of lanthanide dependences, including some deoxyribozymes that strongly favor one particular lanthanide ion (*e.g.*, $Ce^{3+} \gg Eu^{3+} \gg Yb^{3+}$) and others that function well with more than one lanthanide ion. Intriguingly, two of the Yb^{3+}-dependent deoxyribozymes function well with Yb^{3+} alone ($K_{d,app} \sim 10$ μM, in the absence of Zn^{2+}) and have little or no activity with Eu^{3+} or Ce^{3+}. In contrast to these selection outcomes when lanthanide ions were present, new selections with Zn^{2+} or Mn^{2+} alone, or Zn^{2+} with Mg^{2+}/Ca^{2+}, led primarily to deoxyribozymes that cleave DNA by deglycosylation and β-elimination rather than by hydrolysis, including several instances of depyrimidination. We conclude that lanthanide ions warrant closer attention as cofactors when identifying new nucleic acid catalysts, especially for applications in which high concentrations of polyvalent metal ion cofactors are undesirable.

Introduction

Deoxyribozymes are specific DNA sequences that catalyze chemical reactions.[1–3] They are identified by *in vitro* selection[4,5] and generally require one or more divalent metal ions as cofactors. Typical metal ion cofactors are Mg^{2+}, Ca^{2+}, Mn^{2+}, and Zn^{2+}.[6] We described deoxyribozymes that catalyze sequence-specific hydrolysis of phosphodiester linkages in single-stranded DNA substrates, leading to 3′-hydroxyl + 5′-phosphate termini (Fig. 1a) with rate enhancement of 10^{12} over the uncatalyzed DNA hydrolysis reaction[7,8] (up to 3×10^{13} in more recent work[9]). DNA hydrolysis is fundamentally interesting; its catalysis by deoxyribozymes may also have practical utility, especially if hydrolysis activity can be expanded to include double-stranded DNA substrates. Our best initial DNA-hydrolyzing deoxyribozyme, 10MD5, requires both Zn^{2+} (optimal 1 mM) and Mn^{2+} ($K_{d,app}$ 5 mM).[7] Partial randomization and reselection of 10MD5 seeking a tolerance of a wider range of pH values led to a quintuple mutant,[10] for which merely two of the five mutations enable the use of Zn^{2+} alone as the catalytic cofactor.[11] We concluded that millimolar Zn^{2+} is likely required for the catalytic mechanism of 10MD5 and its variants, whereas Mn^{2+} has solely structural contributions. Further selection efforts using a combination of Zn^{2+} and Mn^{2+} led to numerous additional DNA-hydrolyzing deoxyribozymes, including many broadly general DNA catalysts that have very modest sequence requirements for their DNA substrates.[9]

Because Mn^{2+} is redox-active and DNA is sensitive to oxidative degradation,[12–15] we would like to identify new deoxyribozymes that do not require Mn^{2+} for their hydrolytic function. Toward this goal, here we evaluated the ability to identify entirely new DNA-hydrolyzing deoxyribozymes by *in vitro* selection using Zn^{2+} alone or in combination with several other metal ions, including lanthanide ions (Mn^{2+} alone was also evaluated). Trivalent lanthanide ions bind very tightly to nucleic acids[16] and have been reported as alternative catalytic cofactors for a particular RNA-cleaving DNA enzyme originally identified to require Pb^{2+}.[17] The luminescent lanthanides Eu^{3+} and Tb^{3+} have also been used as structural and mechanistic probes for nucleic acids;[17–21] identification of new lanthanide-dependent deoxyribozymes could therefore simplify their biochemical characterization. *Via* new experiments, here we found that the combination of Zn^{2+} with micromolar concentrations of a lanthanide ion (Ce^{3+}, Eu^{3+}, or Yb^{3+}) readily enables *in vitro* selection for DNA phosphodiester hydrolysis, and the resulting deoxyribozymes strictly require lanthanide ions, including two instances of DNA catalysts that each function with 10 μM Yb^{3+} as the sole polyvalent metal ion cofactor. In contrast, use of Zn^{2+} alone (or Zn^{2+} with Mg^{2+}/Ca^{2+}) or Mn^{2+} alone leads primarily to

Department of Chemistry, University of Illinois at Urbana-Champaign, 600 South Mathews Avenue, Urbana, IL 61801, USA. E-mail: scott@scs.illinois.edu

† Electronic supplementary information (ESI) available: additional experimental details. See DOI: 10.1039/c2sc01067d

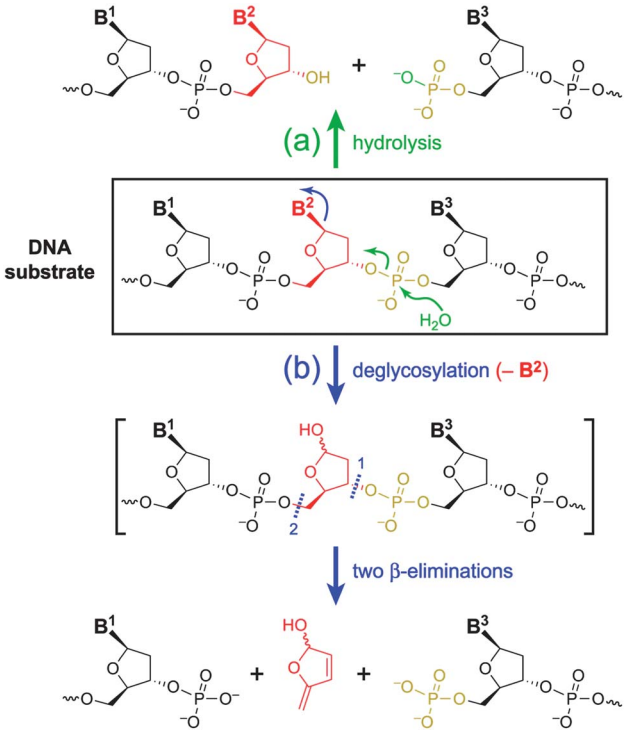

Fig. 1 Two pathways for DNA cleavage. (a) Hydrolysis, leading to either 3′-hydroxyl + 5′-phosphate termini (shown) or 3′-phosphate + 5′-hydroxyl termini (not shown). (b) Deglycosylation followed by strand scission *via* two β-elimination reactions, leading to 3′-phosphate +5′-phosphate termini and a "missing" nucleoside. B = nucleobase.

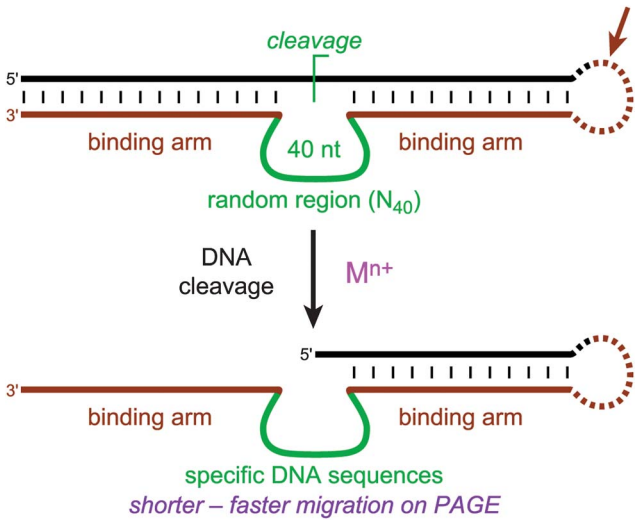

Fig. 2 *In vitro* selection strategy to identify deoxyribozymes that cleave DNA. Depicted is the key selection step, in which catalytically active DNA sequences (along with suitable metal ion cofactors) lead to shorter deoxyribozyme-product conjugates that migrate more quickly on PAGE. These DNA sequences are amplified by PCR and ligated to the uncleaved DNA substrate using T4 RNA ligase (brown arrow) before the next round's selection step. The dotted loop is dispensable for catalysis by the resulting deoxyribozymes, which can cleave their DNA substrate intermolecularly (*in trans*). All assays reported in the other figures were *in trans* (single-turnover conditions).

DNA-catalyzed deglycosylation followed by β-elimination to give strand cleavage (Fig. 1b),[22] rather than DNA hydrolysis. This finding of lanthanide-dependent deoxyribozymes demonstrates that these ions have substantial efficacy as obligatory cofactors for new catalytic function by DNA.

Results

DNA-catalyzed DNA hydrolysis in the presence of lanthanide ions

We initiated three parallel *in vitro* selection efforts, using 1 mM Zn^{2+} with 10 μM of one of Ce^{3+}, Eu^{3+}, and Yb^{3+}, which are at the start, middle, and end, respectively, of the lanthanide series. Each selection reaction was performed in 70 mM HEPES, pH 7.5, 150 mM NaCl at 37 °C with 12 h incubation. The general selection strategy depended upon polyacrylamide gel electrophoresis (PAGE) shift after DNA-catalyzed cleavage of the DNA substrate anywhere within its central region (Fig. 2). Each experiment was iterated for numerous selection rounds, leading to substantial DNA cleavage activity (Fig. S1 in the ESI†). After 6 rounds (Ce^{3+}, Yb^{3+}) or 7 rounds (Eu^{3+}), individual deoxyribozymes were cloned and characterized with regard to their products and metal ion requirements.

The three selection experiments with Zn^{2+} and one of Ce^{3+}, Eu^{3+}, and Yb^{3+} were arbitrarily designated YJ, YK, and YL, respectively, according to our laboratory's systematic alphabetical notation. For all three of these selection experiments, all of the individual deoxyribozymes (see sequences in Fig. S2 in the ESI†) were found to require lanthanide ions (Fig. 3) and to catalyze site-specific DNA hydrolysis (Fig. 4; see comprehensive data in Figs. S3–S5 in the ESI†). These assays were all performed in the presence of 1 mM Zn^{2+} and 10 μM of the relevant lanthanide ion. The two deoxyribozymes identified by selection with Zn^{2+} + Ce^{3+} both had strong catalytic activity with Ce^{3+}, trace activity with Eu^{3+} (63-fold and 15-fold lower k_{obs}), and no detectable activity with Yb^{3+} (Fig. 3a, b). The three DNA catalysts identified with Zn^{2+} + Eu^{3+} had good activity with Eu^{3+} and one or both of the other two tested lanthanide ions (Fig. 3c). Finally, three of the four deoxyribozymes found with Zn^{2+} + Yb^{3+} worked only with Yb^{3+}; the fourth had trace activity with Eu^{3+} as well (Fig. 3d). The specific hydrolysis site within the DNA substrate varied for the different deoxyribozymes (Fig. 4a); in all cases, the hydrolytic nature of the cleavage reaction was confirmed by MALDI mass spectrometry (Fig. 4b, Figs. S3–S5 and Table S2 in the ESI†). The optimal lanthanide ion concentration for each new deoxyribozyme was ~10 μM, as evaluated with the lanthanide ion used during the selection process along with 1 mM Zn^{2+} (Figs. S6–S9 in the ESI†). Structural and mechanistic studies of all of these new deoxyribozymes—which will require considerable future work, given the lack of structural data on any active deoxyribozymes[23]—are anticipated to provide key insights into the catalytic process.

All nine of the new lanthanide-dependent deoxyribozymes were then separately assayed with the lanthanide ion as the sole polyvalent metal ion cofactor, in the absence of Zn^{2+} despite its presence during selection (50 mM HEPES, pH 7.5, 150 mM NaCl, 37 °C). Both of the Ce^{3+}-dependent deoxyribozymes, all three of the Eu^{3+}-dependent DNA enzymes, and two of the four

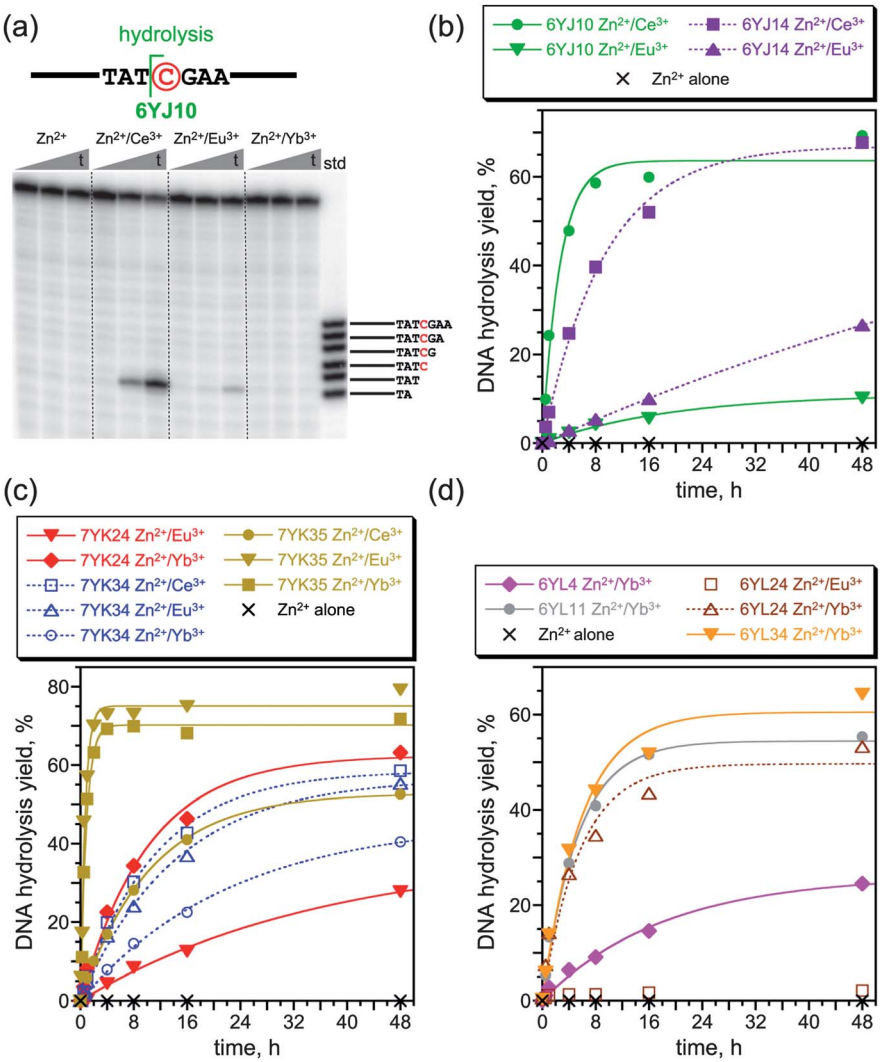

Fig. 3 Activities and lanthanide ion requirements of newly identified deoxyribozymes that catalyze hydrolysis of single-stranded DNA, as identified by *in vitro* selection in the presence of Zn^{2+} and one of Ce^{3+}, Eu^{3+}, or Yb^{3+}. (a) Representative PAGE assay for the 6YJ10 deoxyribozyme, which was identified by selection using Zn^{2+} + Ce^{3+}. Assays were in 70 mM HEPES, pH 7.5, 1 mM $ZnCl_2$, 10 μM of one of $CeCl_3$, $EuCl_3$, or $YbCl_3$, and 150 mM NaCl at 37 °C. Representative timepoints at t = 30 s, 1 h, and 16 h under single-turnover conditions (10 nM 5′-^{32}P-radiolabelled substrate and 1 μM deoxyribozyme). In all cases, the assigned hydrolysis sites were consistent with the PAGE standard ladders (see Experimental Section), while the mass spectrometry data (Fig. 4) allowed truly conclusive assignment of product identities. The circled C nucleotide of the substrate was unpaired in the deoxyribozyme-substrate complex; all other substrate nucleotides were base-paired with the deoxyribozyme's binding arms according to the design of Fig. 2. (b–d) Kinetic plots for deoxyribozymes from the selections with Zn^{2+} + Ce^{3+}, Eu^{3+}, and Yb^{3+}, assayed with the same metal ion combinations and incubation conditions as for 6YJ10 in panel a. k_{obs} values from the first-order curve fits are collected in Table S1 in the ESI†.

Yb^{3+}-dependent DNA catalysts had no detectable activity without Zn^{2+}, even when 40 mM Mg^{2+} was included to maintain high ionic strength (data not shown). However, two of the Yb^{3+}-dependent deoxyribozymes, 6YL4 and 6YL24, had substantial activity with Yb^{3+} alone in the absence of Zn^{2+}, similar in each case to the activity with Yb^{3+} in the presence of Zn^{2+} (Fig. 5; compare Fig. 3d). These Yb^{3+}-only activities were maintained in the presence of 40 mM Mg^{2+} (data not shown). Catalysis by both 6YL4 and 6YL24 was achieved by Yb^{3+} alone (no Zn^{2+}) with $K_{d,app}$ on the order of 10 μM, whereas Eu^{3+} was much less effective and Ce^{3+} did not support detectable activity; loss of activity was observed at higher Yb^{3+} concentrations (Fig. 5 and Figs. S7–S9 in the ESI†). The ratio of k_{obs} values with Yb^{3+} *versus* Eu^{3+} (*i.e.*, the selectivity for Yb^{3+} over Eu^{3+}) was 25-fold and 16-fold, respectively, for 6YL4 and 6YL24.

Because of the prior report of a Pb^{2+}-dependent DNA enzyme that can use lanthanide ions in place of Pb^{2+},[17,24] for each of the new deoxyribozymes we also evaluated replacement of the lanthanide ion with 1 mM Pb^{2+}, either with or without the additional inclusion of Zn^{2+}; in all cases, no activity was observed (data not shown). Also, because each of Ce^{3+}, Eu^{3+}, and Yb^{3+} have accessible +2 oxidation states,[25] we checked the activities of each of the nine new lanthanide-dependent deoxyribozymes with La^{3+}, Gd^{3+}, and Lu^{3+}, each of which is adjacent to one of Ce^{3+}, Eu^{3+}, or Yb^{3+} (respectively) but cannot readily access its +2 oxidation state. In all cases, substantial DNA

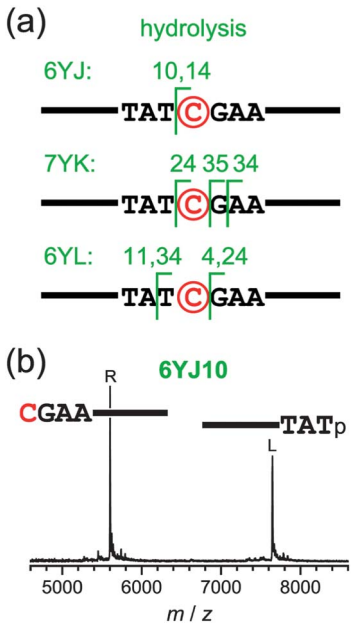

Fig. 4 Hydrolysis sites and mass spectrometry data for the new lanthanide-dependent DNA-hydrolyzing deoxyribozymes. (a) Hydrolysis sites observed for each of the new deoxyribozymes, mapped onto the DNA substrate sequence. All of these new deoxyribozymes create 3′-phosphate + 5′-hydroxyl termini except for one of the Eu^{3+} clones, 7YK34, which leaves 3′-hydroxyl + 5′-phosphate termini. The circled C nucleotide of the substrate was unpaired in the deoxyribozyme-substrate complex. (b) Representative MALDI mass spectrometry data for the products formed by the 6YJ10 deoxyribozyme, validating DNA hydrolysis (L: calcd. 7648.0, found 7648.0, $\Delta = 0$; R: calcd. 5603.7, found 5602.4, $\Delta = -0.02\%$). Analogous data for each of the new lanthanide-dependent deoxyribozymes supported the assigned hydrolysis sites (Table S2 in the ESI†).

hydrolysis activity was retained (data not shown), indicating that the catalysis does not depend upon accessing the lanthanide +2 oxidation state.

DNA-catalyzed DNA hydrolysis in the absence of lanthanide ions

Separately, we performed *in vitro* selection experiments using either 1 mM Zn^{2+} alone or 20 mM Mn^{2+} alone, without any lanthanide ions. Each selection reaction was performed in 70 mM (Zn^{2+}) or 50 mM (Mn^{2+}) HEPES, pH 7.5, 150 mM NaCl at 37 °C with 12 h incubation. From the selection experiment with Mn^{2+} alone (see Fig. S1 in the ESI†), all four new deoxyribozymes were found to catalyze deglycosylation followed by strand scission *via* two β-elimination reactions, which results in loss of a single nucleoside and formation of 3′-phosphate + 5′-phosphate termini (Fig. 1b).[22] The deglycosylation reactions were not uniformly site-specific. Two of the four Mn^{2+}-dependent deoxyribozymes, 8YM17 and 8YM26, catalyzed deglycosylation at either a T or an adjacent A of the DNA substrate, as validated by MALDI mass spectrometry (Fig. 6 and Table S3 in the ESI†). A third deoxyribozyme, 8YM20, deglycosylated at each of three consecutive purines (GAA). The fourth deoxyribozyme, 8YM4, deglycosylated site-specifically at a single G nucleotide.

From the selection experiment with Zn^{2+} alone (see Fig. S1 in the ESI†), one of the five emergent deoxyribozymes, 7YE11, was found to catalyze DNA hydrolysis (Fig. 7a). The other four deoxyribozymes from this selection experiment all induce deglycosylation at either a G or an adjacent A, with mass spectrometry evidence for partial destruction of the deglycosylated nucleoside's sugar ring after the first β-elimination reaction (Fig. S10 in the ESI†). The detailed structure of the final products and their mechanisms of formation are not determined by the available data. Analogous selection experiments were also performed using 1 mM Zn^{2+} and 40 mM of either Mg^{2+} or Ca^{2+} (see Fig. S1 in the ESI†), leading to six (Zn^{2+} + Mg^{2+}) and five (Zn^{2+} + Ca^{2+}) new deoxyribozymes. One of these deoxyribozymes, 8YG11 as identified with Zn^{2+} + Ca^{2+}, catalyzes DNA hydrolysis (Fig. 7b). All ten of the other deoxyribozymes catalyze deglycosylation, of purines alone in the case of Zn^{2+} + Mg^{2+} (Fig. S11 in the ESI†) and of either purines alone or pyrimidines alone in the case of Zn^{2+} + Ca^{2+} (Fig. S12 in the ESI†).

We previously identified a deoxyribozyme that catalyzes oxidative depurination of its own 5′-terminal guanosine residue, requiring periodate as a cofactor.[26] In contrast, the present results demonstrate non-oxidative internal deglycosylation. We speculate that the new lanthanide-independent deoxyribozymes that cleave DNA *via* deglycosylation actively catalyze the deglycosylation step of Fig. 1b, whereas the two subsequent β-elimination reactions that cleave the DNA strand occur spontaneously. The large Mg^{2+}-dependent deoxyribozyme that was identified by Joyce and coworkers to catalyze guanosine depurination[22] was shown to catalyze the depurination step; the subsequent β-elimination reactions were spontaneous, albeit slow, and they could be forced to completion by treatment with base (*e.g.*, piperidine). Here, base treatment did not increase the DNA cleavage yield for any of ten tested deoxyriboyzmes (Fig. S13 in the ESI†). The more facile β-eliminations observed in the present study may relate to the different metal ions that were used.

Discussion

Lanthanide-dependent DNA hydrolysis

In this study, we showed that inclusion of 10 μM of a trivalent lanthanide ion (Ce^{3+}, Eu^{3+}, or Yb^{3+}) along with Zn^{2+} during *in vitro* selection enables consistent identification of strictly lanthanide-dependent deoxyribozymes that hydrolyze single-stranded DNA phosphodiester linkages. Seven of the nine new deoxyribozymes require 1 mM Zn^{2+} in addition to 10 μM lanthanide ion, with clear selectivity for certain lanthanide ions in most but not all cases. Strikingly, two of the new deoxyribozymes, 6YL4 and 6YL24, can use 10 μM Yb^{3+} as the *only* obligatory polyvalent metal ion cofactor, in the absence of Zn^{2+} or any other polyvalent metal ion. The two orders of magnitude concentration difference between 10 μM lanthanide and 1 mM Zn^{2+} may enable new applications of deoxyribozymes, particularly in contexts where high polyvalent metal ion concentrations must be avoided. Future efforts should pursue direct identification of new deoxyribozymes that require only lanthanide ions by including lanthanides as the sole

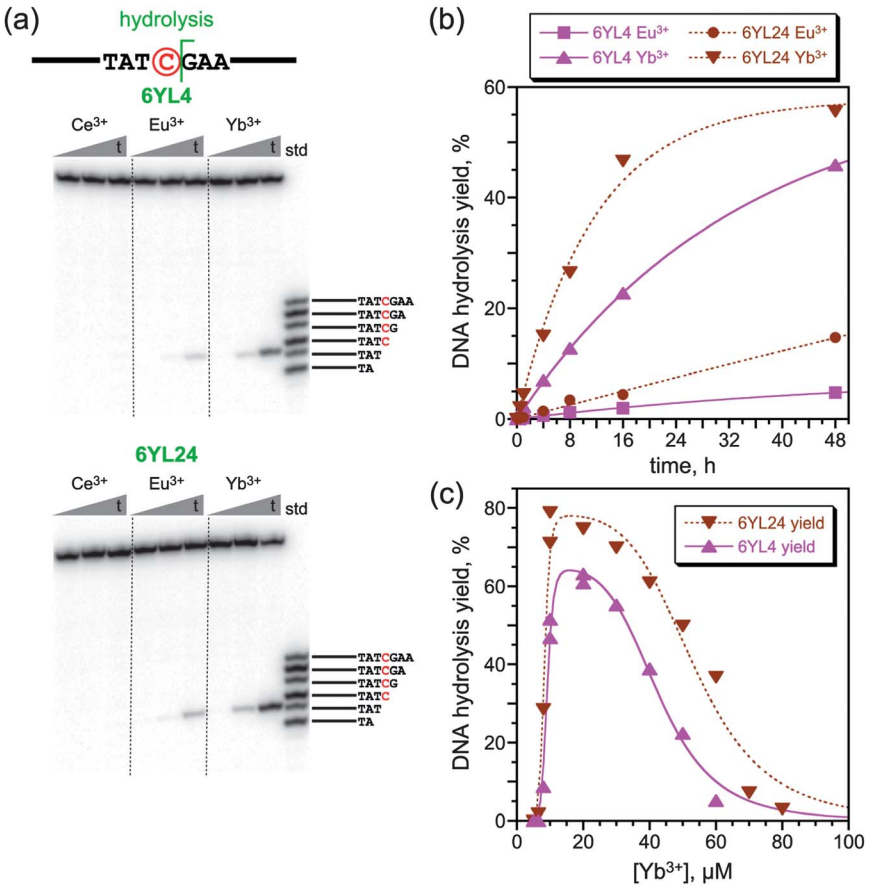

Fig. 5 DNA-catalyzed hydrolysis by the 6YL4 and 6YL24 deoxyribozymes, which are active with Yb^{3+} as the sole polyvalent metal ion cofactor. (a) PAGE assays in 50 mM HEPES, pH 7.5, 10 μM $YbCl_3$, and 150 mM NaCl at 37 °C. Representative timepoints at $t = 30$ s, 1 h, and 16 h under single-turnover conditions (10 nM 5′-^{32}P-radiolabelled substrate and 1 μM deoxyribozyme). The hydrolysis sites are the same as depicted in Fig. 4a for the same DNA enzymes; see MALDI mass spectrometry data in Fig. S5 in the ESI†. The circled C nucleotide of the substrate was unpaired in the deoxyribozyme-substrate complex. When assays were performed at different HEPES concentrations, strong activity was observed at 15–50 mM HEPES, whereas greatly reduced activity was observed at >50 mM HEPES (data not shown). (b) Kinetic plots. For 6YL4, $k_{obs} = 0.038 \pm 0.009$ h^{-1} and yield at 48 h = 48 ± 3% (mean ± sd, $n = 4$). For 6YL24, $k_{obs} = 0.057 \pm 0.020$ h^{-1} and yield at 48 h = 71 ± 11% (mean ± sd, $n = 4$). (c) Dependence of 6YL4 and 6YL24 activity on Yb^{3+} concentration, as quantified by yields at 48 h (data are from a different experiment than in panel b). Each data set was fit to $Y = Y_{max} \cdot [C^n/(K_{activ}{}^n + C^n)] \cdot [1 - C^m/(K_{inhib}{}^m + C^m)]$, where Y = yield, C = Yb^{3+} concentration, K_{activ} and K_{inhib} are apparent binding constants for Yb^{3+} activation and inhibition, respectively, and n and m are Hill coefficients for Yb^{3+} binding and activation, respectively. This equation was derived from a model in which n activating Yb^{3+} ions must bind for the deoxyribozyme to adopt a productive conformation for catalysis, whereas m inhibitory Yb^{3+} ions must *not* bind for the deoxyribozyme to adopt a productive conformation, and moreover, binding of the n activating and m inhibitory Yb^{3+} ions are independent events (and therefore the relevant probabilities multiply). Fit values were as follows: 6YL4 Y_{max} 62%, K_{activ} 9 μM, K_{inhib} 44 μM, n 14, m 6; 6YL24 Y_{max} 75%, K_{activ} 8 μM, K_{inhib} 55 μM, n 14, m 6. The precise numerical values are less important than the overall finding that data for both deoxyribozymes are fit well by a simple model in which Yb^{3+} activation is highly cooperative with ~10 μM apparent binding constant and Yb^{3+} inhibition is somewhat less cooperative with several-fold higher apparent binding constant. We cannot discount the possibility that the "inhibition" observed at high Yb^{3+} concentration is instead a nonspecific effect due to Yb^{3+} precipitation or aggregation rather than true inhibition *via* binding of Yb^{3+} to the deoxyribozyme. However, we have no particular evidence for Yb^{3+} precipitation or aggregation, and others have probed deoxyribozyme activity with lanthanide ions at concentrations considerably higher than we have used here (up to 1.5 mM at pH 7.0).[17]

polyvalent metal ions present during the selection process. Efforts that include increased time pressure for faster reactivity may also be beneficial, considering that most of the new deoxyribozymes have half-lives on the order of several hours, although the fastest lanthanide-dependent deoxyribozymes have half-lives of *ca.* 0.5 h (Table S1 in the ESI†).

The sharp dependence of many of the new deoxyribozymes upon the lanthanide ion identity is remarkable, considering that the primary difference among the evaluated ions is simply their size (radii for hexacoordinate metal ions: Ce^{3+} 102 pm; Eu^{3+} 95 pm; Yb^{3+} 86 pm).[25] In general, on the basis of our overall findings, lanthanide ions deserve closer attention as metal ion cofactors when developing new nucleic acid catalysts. In the context of our recent efforts that revealed DNA-hydrolyzing deoxyribozymes which depend simultaneously upon Zn^{2+} and Mn^{2+},[7,9] as well as our subsequent identification of a particular mutant deoxyribozyme that functions with Zn^{2+} alone,[10,11] the present results have also prompted us to develop new *in vitro* selection strategies for DNA-catalyzed phosphodiester hydrolysis that cannot be subverted by deglycosylation, as was observed here when lanthanide ions were omitted. Such efforts are underway.

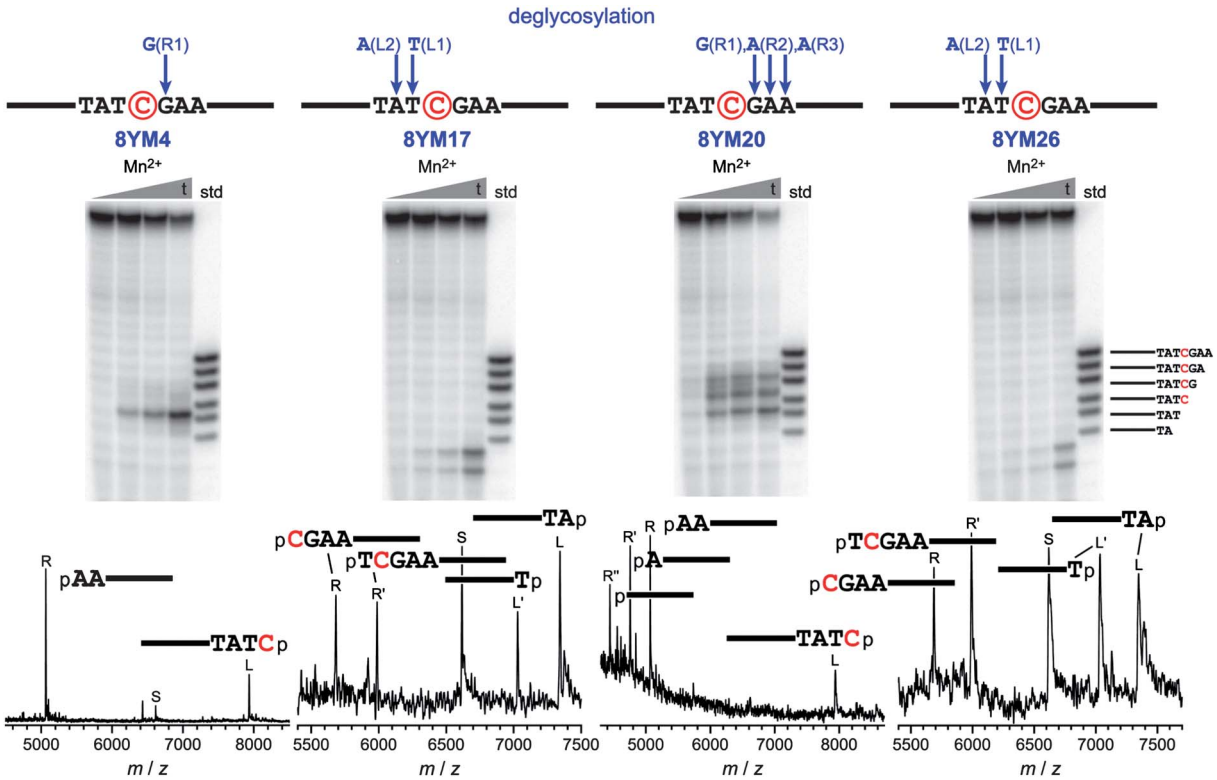

Fig. 6 DNA-catalyzed DNA cleavage by deglycosylation and β-elimination (mechanism of Fig. 1b), illustrated with data for the newly identified Mn^{2+}-dependent deoxyribozymes. Assays were in 50 mM HEPES, pH 7.5, 20 mM $MnCl_2$, and 150 mM NaCl at 37 °C. Representative timepoints at $t = 30$ s, 30 min, 2 h and 16 h under single-turnover conditions. The arrows above each sequence mark the site(s) of deglycosylation, as assigned on the basis of the MALDI mass spectrometry data. Nucleotides are numbered as part of either the L (left) or R (right) portion of the substrate, counting outward. The circled C nucleotide of the substrate was unpaired in the deoxyribozyme-substrate complex. See Table S3 in the ESI† for all mass spectrometry data values. Mass spectrometry peaks labelled S correspond to uncleaved substrate ($z = 2$). In all cases, the assigned deglycosylation sites were consistent with the PAGE standard ladders (see Experimental Section).

Lanthanide-independent DNA cleavage

For the DNA-cleaving deoxyribozymes that were identified by selection in the presence of Mn^{2+} alone, Zn^{2+} alone, or Zn^{2+} with Mg^{2+}/Ca^{2+}, deglycosylation was primarily observed, with hydrolysis (Fig. 7) found for only two out of the 20 characterized DNA enzymes. On the basis of our previous finding that the 10MD5 Zn^{2+}/Mn^{2+}-dependent DNA-hydrolyzing deoxyribozyme could be transformed into a DNA catalyst that requires Zn^{2+} alone by only two mutations,[11] we initially expected that selection with Zn^{2+} alone (or additionally with Mg^{2+} or Ca^{2+}) would readily provide new DNA-hydrolyzing deoxyribozymes. However, the experimental data demonstrate otherwise, *via* the identification instead of primarily DNA-deglycosylating deoxyribozymes. This outcome serves to emphasize the importance of the lanthanide ions in leading reliably to DNA-catalyzed DNA hydrolysis, at least in the present context.

Observation of deglycosylation at multiple positions of the DNA substrate, especially for both purine and pyrimidine nucleotides in the same substrate (*e.g.*, 8YM17 or 8YM26; Fig. 6), suggests a deglycosylation mechanism that is indifferent to the structure of the nucleobase, but more studies are needed to probe these mechanism(s). The finding of depyrimidination (at T or C) rather than depurination (at A or G) by 8YM17 and 8YM26 (Fig. 6) as well as several of the Zn^{2+}/Ca^{2+}-dependent deoxyribozymes (Fig. S12 in the ESI†) is especially curious. Depyrimidination is generally more difficult to catalyze than depurination, because pyrimidine nucleobases lack the purine N7 atom that can be protonated or otherwise activated to assist deglycosylation.[27,28] Although the uncatalyzed deglycosylation rates of purine and pyrimidine nucleosides in DNA are similar[28,29] and uracil DNA glycosylase is well known for damage repair,[30–35] natural enzymatic examples of depyrimidination of cytidine or its analogues are rare.[28,36,37] The observation of DNA-catalyzed deglycosylation at pyrimidine nucleotides further highlights the catalytic competence of DNA.

Experimental section

Oligonucleotides and *in vitro* selection

Oligonucleotides were prepared by solid-phase synthesis at Integrated DNA Technologies (Coralville, IA) and purified by denaturing 20% or 8% PAGE. To avoid unwanted chelation of Zn^{2+} or lanthanide ions by adventitious EDTA, all substrates used in kinetic assays were extracted from gels using TN buffer (10 mM Tris, pH 8.0, 300 mM NaCl) lacking EDTA and precipitated with ethanol. The DNA substrate sequences during the selection process were 5′-CTACCTTTATGCGTATC GAAGGAGGCTTTCGgga-3′, where the 3′-terminal gga

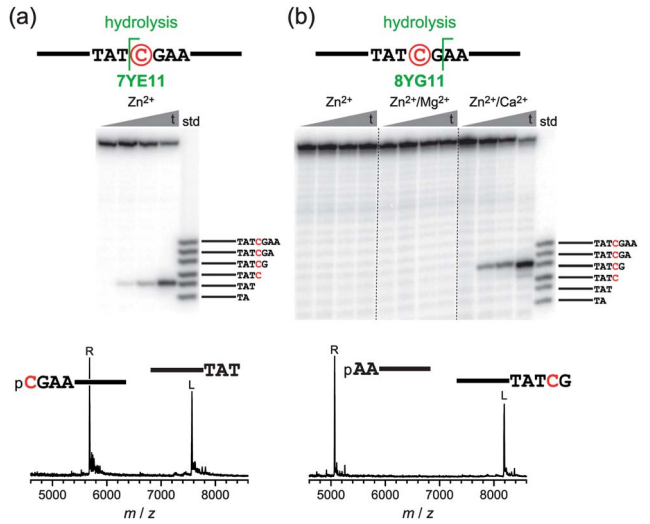

Fig. 7 DNA hydrolysis by two deoxyribozymes identified in the absence of lanthanide ion cofactors. Representative timepoints at $t = 30$ s, 30 min, 2 h and 16 h under single-turnover conditions. (a) 7YE11 deoxyribozyme, identified with Zn^{2+} alone. (b) 8YG11 deoxyribozyme, identified with $Zn^{2+} + Ca^{2+}$. Acquisition and presentation of data is similar to that shown in Fig. 3 and Fig. 4 (1 mM $ZnCl_2$ and, if included, 40 mM $MgCl_2$ or $CaCl_2$). Both deoxyribozymes leave 3′-hydroxyl +5′-phosphate termini in the hydrolysis products. See Table S2 in the ESI† for all mass spectrometry data values.

residues were RNA rather than DNA to enable ligation of the substrate to the deoxyribozyme pool strand by T4 RNA ligase during each selection round. The DNA substrate sequences used for cleavage assays were the same as those used during selection, except the 3′-terminal –gga was replaced with –GGA (*i.e.*, all DNA). The deoxyribozyme pool strand during selections was 5′-CGAA**CGAAAGCCTCCTTC**-N_{40}-**ATACGCATAAAGGTAG** AGCTGATCCTGATGG-3′, where the two bold regions denote the substrate binding arms. The 5′-CGAA was replaced with 5′-CC for individual deoxyribozymes prepared by solid-phase synthesis and used in the single-turnover *in trans* assays. The two PCR primers used during selection were 5′-CGAAC GAAAGCCTCCTTC-3′ (5′-phosphorylated to allow ligation of the product by T4 RNA ligase) and 5′-$(AAC)_4$XCCATCAG GATCAGCT-3′ (where X denotes Glen Spacer 18, which is a PEG spacer that stops extension by Taq polymerase and leads to a size difference between the two PCR product strands).

The *in vitro* selection experiments were performed essentially as described previously[38,39] using 200 pmol ($\sim 10^{14}$ molecules) of DNA in each initial round of selection, where sequence space encompasses $4^{40} \approx 10^{24}$ possibilities (10^{-10} sampling of sequence space). During the key DNA hydrolysis step of each selection round, the sample was incubated at 37 °C for 12 h. Samples that included Zn^{2+} and a lanthanide ion contained 70 mM HEPES, pH 7.5, 1 mM $ZnCl_2$, 10 μM $LnCl_3$, and 150 mM NaCl, where Ln = Ce, Eu, or Yb, in the form of $CeCl_3 \cdot 7H_2O$ (Aldrich 99.9%), $EuCl_3 \cdot 6H_2O$ (Acros 99.99%), or $YbCl_3 \cdot 6H_2O$ (GFS 99.99%). Lanthanide ion stocks were 100 mM $LnCl_3$ and 200 mM HNO_3, diluted with H_2O to 5× relative to the final desired concentration (due to the low final lanthanide ion concentration, the small HNO_3 concentration contributed to the final sample was negligible relative to the much higher HEPES buffer concentration). Samples that included Zn^{2+} either alone or with Mg^{2+}/Ca^{2+} contained 70 mM HEPES, pH 7.5, 1 mM $ZnCl_2$, 40 mM $MgCl_2$ or $CaCl_2$ if appropriate, and 150 mM NaCl. The Zn^{2+} was added from a 10× stock of 10 mM $ZnCl_2$ in 20 mM HNO_3 and 200 mM HEPES, pH 7.5, this 10× stock was itself prepared from a solution of 100 mM $ZnCl_2$ in 200 mM HNO_3 and a solution of 1 M HEPES, pH 7.5.[40] Samples that included Mn^{2+} contained 50 mM HEPES, pH 7.5, 20 mM $MnCl_2$, and 150 mM NaCl.

DNA cleavage assay procedures

The DNA cleavage assays using individual deoxyribozymes were performed under single-turnover *in trans* conditions as described previously.[10] The final incubation conditions were as described above for the selection experiments. The lanthanide ion concentration was 3 to 80 μM. When only lanthanide ions were present (*i.e.*, Zn^{2+} was absent), the HEPES concentration was 50 mM. All assays contained 10 nM 5′-^{32}P-radiolabelled DNA substrate and 1 μM deoxyribozyme (1 : 100) in 10–25 μL total volume. Assay samples were separated by 20% PAGE and quantified with a PhosphorImager. Values of k_{obs} and final yield were obtained by fitting the data directly to first-order kinetics, or to initial-rate kinetics when necessary.

On each assay gel was loaded the same series of oligonucleotide standards. These standards provide a common reference point for comparing gel images and also provided a basis for preliminary assignment of reaction products, albeit with some ambiguity due to near-coincident migration of (i) oligonucleotides of length n with 3′-hydroxyl with (ii) oligonucleotides of length $n + 1$ with 3′-phosphate (greater mass reduces the migration rate, whereas greater charge increases the migration rate). Because each standard oligonucleotide was synthesized with 3′-hydroxyl rather than 3′-phosphate, there is a vertical offset for each 3′-phosphate product relative to the corresponding 3′-hydroxyl standard band (the product migrates faster than the standard). The definitive assignment of each deoxyribozyme's reaction product was made on the basis of the mass spectrometry data.

Mass spectrometry

Samples for mass spectrometry were prepared as follows. A 100 μL sample containing 60 pmol of substrate and 200 pmol of deoxyribozyme was annealed in 5 mM HEPES, pH 7.5, 15 mM NaCl, and 0.1 mM EDTA (the EDTA was omitted for lanthanide-containing reactions) by heating at 95 °C for 3 min and cooling on ice for 5 min. The cleavage reaction was initiated by addition of stock solutions to a final volume of 200 μL containing HEPES, pH 7.5, and metal ions as described above for *in vitro* selection. The sample was incubated at 37 °C for 16 h. The nucleic acids were precipitated by adding 20 μL of 3 M NaCl and 660 μL of ethanol and dissolved in 40 μL water. The sample was desalted in 10 μL portions using four C_{18} ZipTips and analyzed by MALDI mass spectrometry with 3-hydroxypicolinic acid as matrix. All MALDI mass spectra were obtained in the mass spectrometry laboratory of the UIUC School of Chemical Sciences. For detailed tables of mass spectrometry data, see Tables S2 and S3 in the ESI†.

Acknowledgements

This research was supported by grants to S.K.S. from the National Institutes of Health (GM065966), the Defense Threat Reduction Agency (HDTRA1-09-1-0011), and the National Science Foundation (0842534). V.D. was partially supported by NIH T32 GM070421.

Notes and references

1 S. K. Silverman, *Chem. Commun.*, 2008, 3467–3485.
2 K. Schlosser and Y. Li, *Chem. Biol.*, 2009, **16**, 311–322.
3 S. K. Silverman, *Angew. Chem., Int. Ed.*, 2010, **49**, 7180–7201.
4 G. F. Joyce, *Annu. Rev. Biochem.*, 2004, **73**, 791–836.
5 G. F. Joyce, *Angew. Chem., Int. Ed.*, 2007, **46**, 6420–6436.
6 S. K. Silverman, *Acc. Chem. Res.*, 2009, **42**, 1521–1531.
7 M. Chandra, A. Sachdeva and S. K. Silverman, *Nat. Chem. Biol.*, 2009, **5**, 718–720.
8 M. I. Fekry and K. S. Gates, *Nat. Chem. Biol.*, 2009, **5**, 710–711.
9 Y. Xiao, R. J. Wehrmann, N. A. Ibrahim and S. K. Silverman, *Nucleic Acids Res.*, 2012, **40**, 1778–1796.
10 Y. Xiao, M. Chandra and S. K. Silverman, *Biochemistry*, 2010, **49**, 9630–9637.
11 Y. Xiao, E. C. Allen and S. K. Silverman, *Chem. Commun.*, 2011, **47**, 1749–1751.
12 C. J. Burrows and J. G. Muller, *Chem. Rev.*, 1998, **98**, 1109–1152.
13 W. K. Pogozelski and T. D. Tullius, *Chem. Rev.*, 1998, **98**, 1089–1107.
14 M. M. Greenberg, *Org. Biomol. Chem.*, 2007, **5**, 18–30.
15 K. S. Gates, *Chem. Res. Toxicol.*, 2009, **22**, 1747–1760.
16 S. J. Franklin, *Curr. Opin. Chem. Biol.*, 2001, **5**, 201–208.
17 C. R. Geyer and D. Sen, *J. Mol. Biol.*, 1998, **275**, 483–489.
18 A. L. Feig, M. Panek, W. D. Horrocks and O. C. Uhlenbeck, *Chem. Biol.*, 1999, **6**, 801–810.
19 M. Komiyama, N. Takeda and H. Shigekawa, *Chem. Commun.*, 1999, 1443–1451.
20 N. G. Walter, N. Yang and J. M. Burke, *J. Mol. Biol.*, 2000, **298**, 539–555.
21 C. Mundoma and N. L. Greenbaum, *J. Am. Chem. Soc.*, 2002, **124**, 3525–3532.
22 T. L. Sheppard, P. Ordoukhanian and G. F. Joyce, *Proc. Natl. Acad. Sci. U. S. A.*, 2000, **97**, 7802–7807.
23 J. Nowakowski, P. J. Shim, G. S. Prasad, C. D. Stout and G. F. Joyce, *Nat. Struct. Biol.*, 1999, **6**, 151–156.
24 R. R. Breaker and G. F. Joyce, *Chem. Biol.*, 1994, **1**, 223–229.
25 N. N. Greenwood and A. Earnshaw, *Chemistry of the Elements*, Butterworth-Heineman: Oxford, 1997, p. 1233.
26 C. Höbartner, P. I. Pradeepkumar and S. K. Silverman, *Chem. Commun.*, 2007, 2255–2257.
27 J. A. Zoltewicz, D. F. Clark, T. W. Sharpless and G. Grahe, *J. Am. Chem. Soc.*, 1970, **92**, 1741–1750.
28 P. J. Berti and J. A. McCann, *Chem. Rev.*, 2006, **106**, 506–555.
29 G. K. Schroeder and R. Wolfenden, *Biochemistry*, 2007, **46**, 13638–13647.
30 T. Lindahl, S. Ljungquist, W. Siegert, B. Nyberg and B. Sperens, *J. Biol. Chem.*, 1977, **252**, 3286–3294.
31 L. C. Olsen, R. Aasland, C. U. Wittwer, H. E. Krokan and D. E. Helland, *EMBO J.*, 1989, **8**, 3121–3125.
32 S. J. Muller and S. Caradonna, *Biochim. Biophys. Acta*, 1991, **1088**, 197–207.
33 C. D. Mol, A. S. Arvai, G. Slupphaug, B. Kavli, I. Alseth, H. E. Krokan and J. A. Tainer, *Cell*, 1995, **80**, 869–878.
34 C. D. Mol, S. S. Parikh, C. D. Putnam, T. P. Lo and J. A. Tainer, *Annu. Rev. Biophys. Biomol. Struct.*, 1999, **28**, 101–128.
35 J. I. Friedman and J. T. Stivers, *Biochemistry*, 2010, **49**, 4957–4967.
36 B. Dalhus, J. K. Laerdahl, P. H. Backe and M. Bjørås, *FEMS Microbiol. Rev.*, 2009, **33**, 1044–1078.
37 Y. G. Mok, R. Uzawa, J. Lee, G. M. Weiner, B. F. Eichman, R. L. Fischer and J. H. Huh, *Proc. Natl. Acad. Sci. U. S. A.*, 2010, **107**, 19225–19230.
38 A. Flynn-Charlebois, Y. Wang, T. K. Prior, I. Rashid, K. A. Hoadley, R. L. Coppins, A. C. Wolf and S. K. Silverman, *J. Am. Chem. Soc.*, 2003, **125**, 2444–2454.
39 D. M. Kost, J. P. Gerdt, P. I. Pradeepkumar and S. K. Silverman, *Org. Biomol. Chem.*, 2008, **6**, 4391–4398.
40 K. A. Hoadley, W. E. Purtha, A. C. Wolf, A. Flynn-Charlebois and S. K. Silverman, *Biochemistry*, 2005, **44**, 9217–9231.